Original Research Article

How Suitable is the Ringsail Parachute to Facilitate the Descent of NASA's Mars Sample Retrieval Lander into the Martian Atmosphere?

Aarushi Sanganeria

Tanglin Trust School, 95 Portsdown Road, Singapore

ABSTRACT

The Mars Sample Retrieval mission demands high-performance parachutes capable of surviving supersonic deceleration in Mars' low-density atmosphere, specifically for the Lander. This study evaluates the suitability of a Ringsail parachute through computational fluid dynamics (CFD) simulations at supersonic (500 ms^{-1}), low density (0.02 kgm^{-3}) conditions. Velocity magnitude analysis revealed significant flow separation and turbulent wake formation. Stagnation zones posed localized stress risks, while asymmetric vorticity suggested susceptibility to collapse. This paper used computational fluid dynamics to evaluate the performance of a Ringsail parachute designed in Fusion360 in Martian atmospheric conditions through analysing lift and drag forces and coefficient of drag. The results are then validated against a previous study regarding the performance of Supersonic Ringsail Parachutes on Mars. Future work could explore transient inflation dynamics, material thermal limits, and varying porosity.

Keywords: Parachute; Ringsail parachute; Martian atmosphere; Sample Retrieval Lander; Lift; Coefficient of drag; CFD

INTRODUCTION

National Aeronautics and Space Administration (NASA)'s Mars Sample Retrieval mission, in cooperation with the European Space Agency (ESA), was approved in September 2022 and has been in the works ever since the landing of Perseverance. Set to launch within the next ten years, it aims to return samples of Mars collected by the Perseverance rover in 2021 (1). Currently, NASA is working on developing the technology that will be used for this mission which involves the Sample Retrieval Lander and the Mars Ascent Vehicle, the two main vehicles that are a part of this rendezvous mission. However, landing spacecraft on Mars presents its own challenges due to its vastly different atmosphere compared to Earth's. Hence, NASA is also improving and adjusting the Entry, Descent and Landing (EDL) system to suit the Sample Retrieval Lander (SRL) (2). NASA's EDL takes into account the thin Martian atmosphere and makes use of Aeroshells, Parachutes, and other decelerators, and has been successful in previous Mars missions such as Perseverance and Curiosity. As the SRL is larger in mass and size than previous payloads in past Mars missions at an expected 3,375 kilograms (1),

Corresponding author: Aarushi Sanganeria, E-mail: aarushi.sanganeria2007@gmail.com.

Accepted October 21, 2025
https://doi.org/10.70251/HYJR2348.3510681077

however, the EDL sequence will differ and require more advanced components, including the parachute, which is instrumental for a successful terminal descent. Indeed, NASA mentioned in their Langley/Ames EDL Seminar Series in summer 2021 that the parachute is required to be 'larger than any past mission' (2). During the development of the EDL, they could potentially test out the applicability of Ringsail parachutes as well, as it may be more suitable for larger mass payloads, a notion proposed and tested by NASA's Low-Density Supersonic Decelerator (LDSD) programme. Especially as the largest mass that has landed on Mars to date is the Perseverance rover, which is still just over three times less the mass of the Sample Retrieval Lander, a parachute more capable of producing high amounts of drag is necessary. Moreover, developing the Ringsail design to perform at supersonic speeds could prevent the need for another Ringsail parachute to be deployed at subsonic speeds, as the same parachute could be used due to the Ringsail's consistent reliable performance in subsonic conditions. This has the potential to reduce costs and mass of the entire system, which are important considerations especially as NASA faces a steep cost for this mission. Therefore, this paper conducted a preliminary test with available data regarding the payload to conclude whether a supersonic Ringsail parachute would be effective in decelerating the SRL during its EDL sequence. Specifically, this paper analysed the drag and lift forces, the coefficient of drag, and stability of the parachute.

LITERATURE REVIEW

The development of parachutes for interplanetary missions began in 1967 when NASA's Langley Research Centre launched the Planetary Entry Parachute Program which aimed to understand the performance of parachutes when launched in supersonic, low-density conditions, similar to those of Mars' atmosphere. This program was a precursor to the Viking Program and was among other programs that developed supersonic decelerators for use in the Viking missions such as the Supersonic Planetary Entry Decelerator Program and Supersonic High-Altitude Parachute Experiment. It consisted of a series of test flights that investigated parachutes' deployment characteristics such as drag and stability (3). Three key shapes of parachutes were tested: the Disk-Gap Band (DGB), Ringsail, and Cross. The Cross parachute was found to have a large drag area but minimum stability and has therefore not been used or considered much for Mars missions. The Ringsail proved to work well for Mach numbers under 1.9, however the DGB proved to be the most suitable with better inflation and decent performance (3).

One of the initial tests which proved the viability of the DGB parachute involved the parachute being deployed in a simulated Martian environment. This involved deploying it at a Mach number of 1.59 and a dynamic pressure of 555 N/m^2. During this flight test, two panels of the disk had torn since there was a collision between the canopy and the bag in which the parachute was stored in, yet despite this, the parachute was successfully able to inflate stably and produce a suitable drag force (4).

The application of parachutes for actual interplanetary missions, specifically Mars, first began with the Viking Program. The program, beginning in 1968, intended to land the first spacecrafts on Mars, Vikings 1 and 2. As a part of this program, various DGB parachute designs were tested to determine the suitability for the Viking landers. The DGB was most likely chosen due to the testing this particular shape had undergone as a part of PEPP prior to this. Their performance when deployed in subsonic (Mach 0.5), transonic (Mach 0.9), and supersonic (Mach 2.2) levels was analysed by the Langley Research Centre (5). Through multiple flight and qualification tests conducted during the 1970s leading up to the launch in 1975, a 16 metre DGB parachute was ultimately chosen. According to a flight test by the Langley Research Centre conducted before the launch in November 1974, the parachute "successfully deployed, inflated, and exhibited sufficient drag and stability for Viking '75 mission requirements." (5).

Since then, the DGB, pictured in Figure 1, has been the parachute of choice for Mars missions, as it has been proven to function well in supersonic, low-density environments, posing lower risks. In particular, its superior stability in supersonic conditions is one major factor behind the use of DGB in Mars missions. It was used in the EDL sequence of the rovers Curiosity and Perseverance and was also deployed in China's Tianwen-1 mission.

Between Mars missions, the design of the DGB has evolved as different missions have different landing requirements. The DGB can mainly be classified into two main subsections: the Viking type and the Mars pathfinder (MPF) type. The Viking type is characterized by its higher drag coefficient yet lower stability, while the MPF type is known for its lower grad coefficient but higher stability (7).

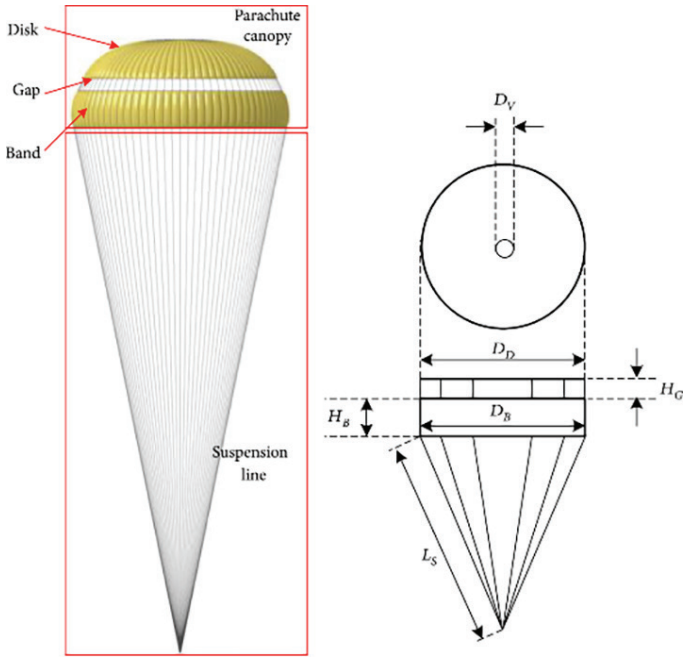

Figure 1. The design and construction parameters of the DGB parachute used for the Tianwen-1 mission. It presents a modelled view of the parachute on the left and the working drawing on the right, labelled with the dimensions. This figure clearly shows the three major components of the parachute, the disk, gap, and the band, giving it its name (6).

Previously, the use of the Ringsail parachute was limited to subsonic deceleration, specifically in Earth's atmosphere, as it has been proven to have a better subsonic drag performance than the DGB. Some notable missions which involved the use of Ringsail parachutes include Apollo, Gemini, and Mercury. In these missions, Ringsail parachutes were used in spacecrafts' return to Earth. Yet there has been limited flight test data for Ringsail parachutes on supersonic environments as no spacecraft landing on Mars have deployed Ringsail parachutes thus far.

In 2014, NASA initiated its LDSD project at its Jet Propulsion Laboratory in order to develop supersonic Ringsail (SSRS) parachutes for larger payloads landing on Mars. It focused on developing a larger diameter SSRS parachute of roughly 30 metres, turning out to be the largest supersonic parachute deployed, and conducted two major test flights. During the first test, the parachute was unable to inflate properly and resulted in a hard landing in the Pacific Ocean (8). Improving from this, NASA tested a second version a year later in 2015 which was able to inflate fully as intended, proving that there is a probable chance for SSRS parachutes to be developed for use on Mars. Following the LDSD Project, a year later, the Advanced Supersonic Parachute Inflation Research Experiments (ASPIRE) project was launched focusing specifically on developing supersonic parachutes for Mars robotic missions. One of its biggest outcomes was developing the parachute used for the Mars 2020 rover, Perseverance.

In a recent numerical study on parachutes systems for Mars exploring fabric permeability and porosity, it was acknowledged that larger payloads exceed 'the maximum allowed one of disk-band-gap parachute' (9). While this research focused on the structural integrity of the parachute, it does provide insights into the possibility of the use of the Ringsail parachute for supersonic deceleration in Mars, suggesting that through considering the structure and how it influences fluid behaviour around the parachute, the Ringsail can be adequately developed for future Mars missions with larger payloads. Therefore, as this is a possibility, this paper assesses the performance of a 24-diameter Ringsail parachute in low-density, supersonic conditions.

METHODS AND MATERIALS

This paper utilised a computational method to analyse the suitability of Ringsail parachutes. First, designs of the Ringsail parachute were created on Autodesk®'s Fusion360 CAD software. This software was used due to its availability for student accounts. The sizes were based on the parachute used for the Perseverance mission, as NASA revealed in their Langley/Ames EDL Seminar Series that the parachute used would be a developed version of the DGB parachute used for Perseverance. As a part of this seminar, they mentioned exploring the use of 24 metre diameter parachutes. Therefore, the parachute was designed with a diameter of 24 metres.

As solely the aerodynamics of the parachute were being assessed, suspension lines between a point representing the payload and the parachute were not included in the design. This is because this paper is solely focused on canopy aerodynamics and the force generated by the canopy, hence removing suspension lines would isolate the canopy shape, Ringsail, as the variable of interest. Suspension lines are constant regardless of canopy shape, hence the drag force produced by them would largely be the same regardless of canopy shape and would not be representative of the drag force produced

by the canopy. Additionally, the drag forces generated by suspension lines would be negligible compared to those generated by the canopy. Therefore, to simplify the design and reduce chances of meshing errors due to increased complexity, suspension lines were omitted. This led to the design visible in Figure 2.

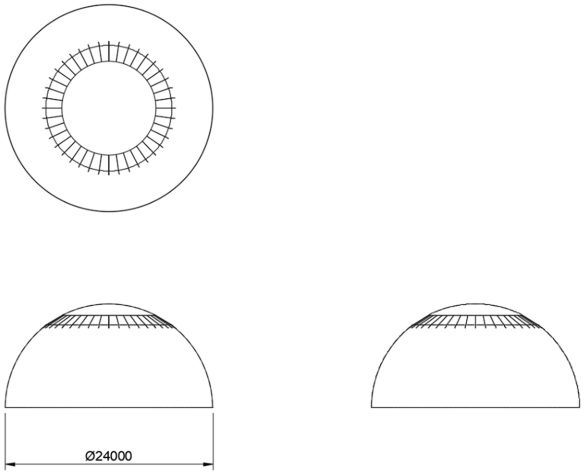

Figure 2. Third angle projection of Ringsail parachute design in Fusion360 CAD software (dimension of the diameter visible in millimetres), presenting the front, plan, and side view of the parachute. The key feature characterising the Ringsail, the vent ring, is visible as a constrained vent with suspension lines across it.

However, it is important to note that this design does not take into account porosity, therefore the CFD simulation will treat it as a solid body. This would lead to results depicting higher drag forces than would be the case with porous fabric, which must be taken into account when analysing data.

After the parachute was designed on Fusion360, it was uploaded onto Autodesk® CFD, a CFD software that facilitates the simulation of objects in fluids. While Autodesk CFD does have certain solver limitations due to its comparatively weaker meshing abilities for complex geometries, this set up has been validated against other studies, such as (10), which provide evidence for Autodesk CFD's accuracy, revealing that it was the most accurate out of the three software tested by the study with a deviation of less than 20% from empirical results. Moreover, its availability for student accounts made it conveniently accessible for this study. However, it should be noted that Autodesk CFD is being used to simulate supersonic flow in this paper, which may lead to larger deviations or errors from actual values, yet this would only affect results and the setup remains largely the same, save for the differences in density, pressure, temperature, velocity, and composition of the fluid.

The conditions of the fluid were adjusted to mimic the thin Martian atmosphere. Figure 3 displays the conditions which define the atmosphere.

Property	Value
Density	0.02 kgm^{-3}
Pressure	610 Pa
Temperature	210 K
Velocity	500 ms^{-1}

Figure 3. The conditions of the carbon dioxide-rich Martian atmosphere that was simulated in the CFD environment. The Martian atmosphere is defined by the key features density (kgm^{-3}), pressure (Pascal), and temperature (Kelvin), and the velocity (ms^{-1}) was input into the CFD as the fluid velocity in order to simulate the velocity of the payload being 500 ms^{-1}.

In Autodesk® CFD, a simulation was run with carbon dioxide, as that makes up 95% of the Martian atmosphere. The specific conditions entered in Autodesk® CFD for the carbon dioxide are the same as the ones shown above in Figure 3. The values for these parameters are either standard values of carbon dioxide or known and commonly accepted values of carbon dioxide on Mars. Moreover, 500 ms^{-1} was chosen as the velocity of the airflow as according to the discussion at the NASA Langley/Ames EDL Seminar Series in summer 2021, the velocity at which parachute deployment will occur is at 500 ms^{-1}, at roughly Mach 2.1, after decelerating from the initial entry interface velocity of 6000 ms^{-1} (2). This means the Lander will be traveling at that velocity before drag force due to the parachute decelerates it, therefore this value was chosen for the CFD simulation.

A wind tunnel was created around the parachute before the simulation was run, seen in Figure 4. Compressible analysis was conducted to allow for simulation of supersonic flow. The velocity inlet was set to 500 ms^{-1}. On Autodesk, the simulation was run for the parachute and data was collected on the lift and drag forces, as well as lateral forces to analyse stability and qualitative data regarding flow of air around the parachute.

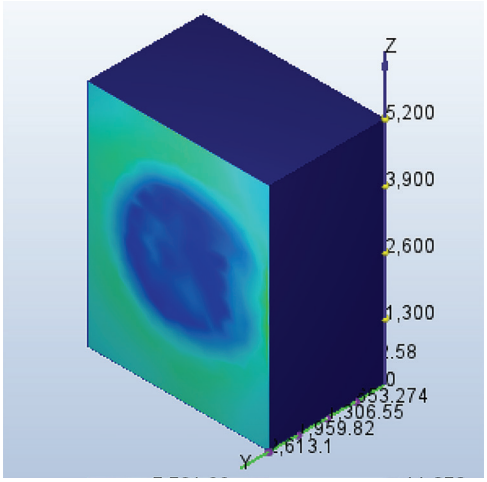

Figure 4. Ringsail parachute in the wind tunnel while Autodesk CFD is running the simulation. This image is taken at the beginning of the simulation. The box represents the wind tunnel, essentially a hollowed out, rectangular body, within which the Ringsail parachute is contained, rotated so that it is in plane with the front and back faces of the wind tunnel. The different colours correspond to the velocities of the fluid at those points. The greener colours represent speeds of around 500-600 ms^{-1}, while dark blue represents 0 ms^{-1}.

RESULTS

The Ringsail parachute reached convergence on Autodesk® CFD after 3,636 iterations. Convergence was detected by Autodesk® CFD's automatic convergence assessment which stops the analysis if there are no significant changes between one iteration and the next. The convergence plot for the Ringsail parachute is shown below in Figure 5, accompanied by the legend for this graph.

In this figure, convergence refers to the stabilization of the residuals and solution variables represented by the curves after roughly 3,600 iterations of airflow. The solver is considered converged when each curve plateaus and the change in the value of all variables between the current and several hundred subsequent iterations is considered negligible. This indicates that the simulation is reaching its true physical state.

Through the wall calculator, the forces on the parachute can be seen below in Figure 6. The direction of the flow of air was parallel to Fy, meaning Fy is the lift/drag force on the parachute.

TOTAL FX, 502559, Newton
TOTAL FY, 4.43085e+06, Newton
TOTAL FZ, -180382, Newton

Figure 6. Forces in each of the 3 axes for the Ringsail parachute, where Fy is the lift/drag force, as this is the force acting on the underside of the canopy, and Fx and Fz are the lateral forces, with Fx representing the forces acting towards the left and the right of the parachute, while Fz represents forces acting up and down on the parachute. As visible in the figure, the units for these forces are Newtons.

The drag force of roughly 4.4MN can be used to calculate the deceleration a of the spacecraft in Mars with Newton's Second Law, using the mass of the Lander m as 3375kg, the value available on NASA's technical specifications for the Lander. The force of drag F_{drag} used was the force in the y-axis in the CFD simulation, and the value of acceleration due to gravity on Mars g_{Mars} was used to calculate the weight W of the Lander.

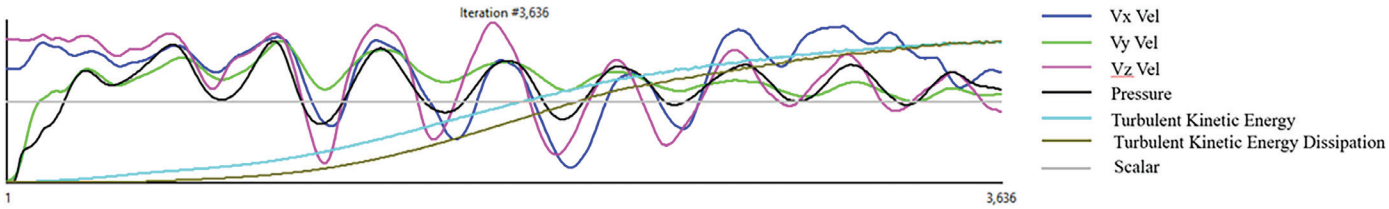

Figure 5. Convergence plot for the Ringsail parachute in Autodesk® CFD including a legend for each curve. This represents the value of each of the components measured at each iteration of the CFD simulation, forming various curves. The velocities are all measured in cms^{-1}, pressure is measured in Pa, turbulent kinetic energy is measured in m^2s^{-2}, and turbulent kinetic energy dissipation in m^2s^{-3}. The curves begin to level off after 3,636 iterations, revealing that the solver has converged.

$F_{drag} = 4.43106MN$

$m = 3375kg$

$g_{Mars} = 3.71ms^{-2}$

$W = mg = 12{,}521N$

$$a = \frac{4.43 \times 10^6 - 1.25 \times 10^4}{3375} = 1308.89ms^{-2}$$

This would mean there is a deceleration of 1308.89 ms^{-2}. The coefficient of drag C_d was then calculated so it can be better compared to other parachutes deployed on Mars. The values substituted for density ρ and velocity u can be found in Figure 3, while A is the reference area.

$$C_d = \frac{2F}{\rho u^2 A}$$

$$C_d = \frac{2 \times 4.43 \times 10^6}{0.02 \times 500^2 \times 467.2}$$

$C_d = 3.79$

This value for the coefficient of drag is significantly higher than necessary for Mars missions. They tend to be roughly 0.5-0.8 (6) for deployment of supersonic DGB parachutes, which is optimal for these missions. As suggested in the Methodology, this abnormally high coefficient of drag is possibly largely due to the large drag force due to the impermeability of the parachute canopy.

Therefore, to find a more accurate estimation for the coefficient of drag of this parachute, porosity was factored in. Simulation data for parachutes in Martian conditions which are not impermeable from studies such as (11) and (12) suggest that the wake velocity of parachutes with porosity is roughly under half of the approach velocity, whilst for impermeable parachutes, the wake velocity is 0 ms^{-1}. This information can be used to find the ratio of dynamic pressure of a porous parachute to the dynamic pressure of an impermeable parachute, which can then be multiplied by the drag force of the impermeable parachute to find an estimate for the drag force acting on a porous parachute. The below equation describes change in dynamic pressure Δq in terms of density and change in velocity, represented by the difference of the wake velocity, v, squared and approach velocity, u, squared.

$$\Delta q = \frac{1}{2}\rho(v^2 - u^2)$$

Since the reference area is constant regardless of porosity, the ratio of dynamic pressure is equal to the ratio of the forces acting on each parachute.

$$\frac{F_{porous}}{F_{impermeable}} = \frac{\Delta q_{porous}}{\Delta q_{impermeable}}$$

Additionally, as density is constant, dynamic pressure can be written as the difference in the wave velocity squared and the approach velocity squared. According to the trends noted in studies (11) and (12), the wave velocity was estimated to be roughly 250 ms^{-1}.

$$\frac{F_{porous}}{F_{impermeable}} = \frac{(v^2 - u^2)_{porous}}{(v^2 - u^2)_{impermeable}}$$

$$\frac{F_{porous}}{4.43 \times 10^6} = \frac{(250^2 - 500^2)_{porous}}{(0^2 - 500^2)_{impermeable}}$$

$$\frac{F_{porous}}{4.43 \times 10^6} = 0.25$$

$$F_{porous} = 0.25 \times 4.43 \times 10^6$$

$$F_{porous} \backsimeq 1.11 \times 10^6$$

Using this estimated value for the drag force of a porous parachute, a more accurate value for the coefficient of drag can be calculated.

$$C_d = \frac{2F}{\rho u^2 A}$$

$$C_d = \frac{2 \times 1.11 \times 10^6}{0.02 \times 500^2 \times 467.2}$$

$C_d \approx 0.95$

This result is closer to the typical range for the drag coefficient of Mars lander parachutes of 0.5-0.8, and is in fact within the range of the drag coefficient for the triconical DGB modification of 0.8-0.96 (6). Once quantitative data of the parachute was produced and analysed, the performance of the parachute canopy was also analysed qualitatively through airflow data.

As visible in Figure 7, the parachute massively decelerated the air, seen by the dark blue wake of the parachute. The highest velocities occur near the edges of the parachute, represented by the green regions, which are around two times larger than the inlet velocity of 500 ms^{-1}), suggesting high-speed flow separation. This may be one of the main reasons for the significant lateral forces mentioned in Figure 6. There are some regions with velocities of 0 ms^{-1} near the parachute surface, suggesting stagnation points. Moreover, as visible on the underside of the canopy, the velocity is roughly 200 ms^{-1}, suggesting that due to the impermeability of this

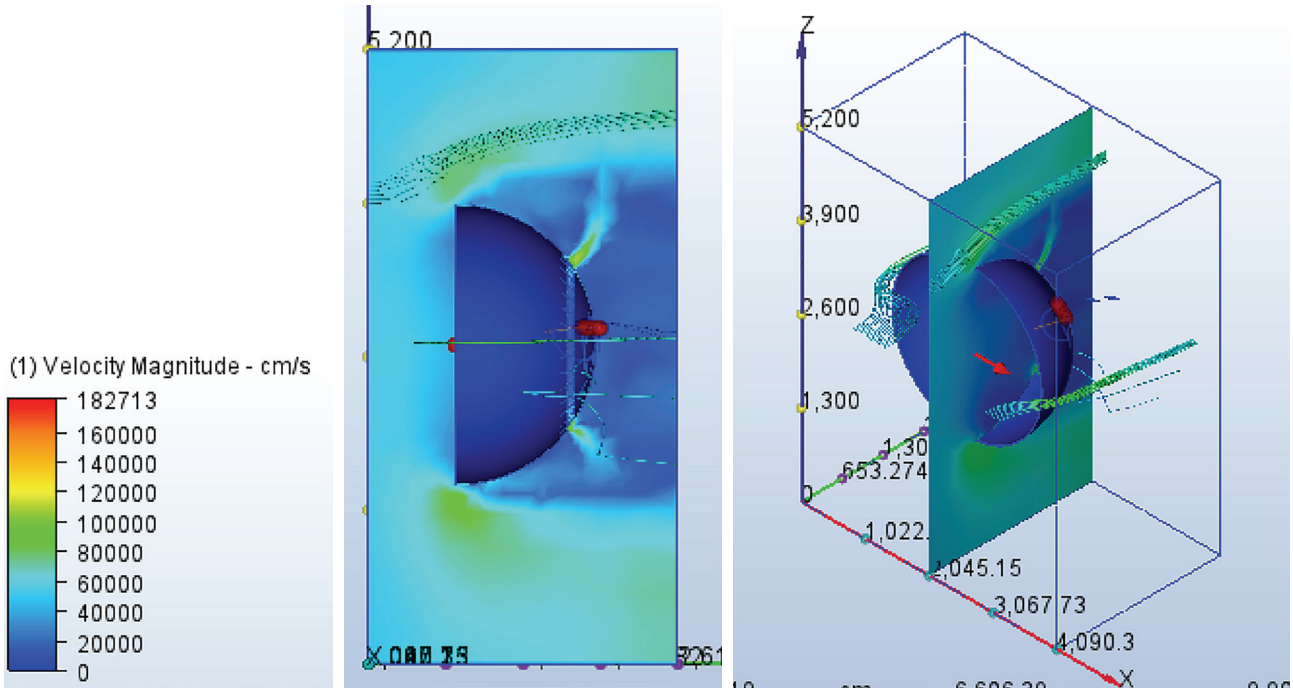

Figure 7. In the middle, the plane represents the flow of air through the middle of the parachute. On the right, the model shows the flow of air around the sides of the parachute. The left shows the key to understanding the blue and green colours, which represent the velocities of the fluid at different positions on the parachute in cms^{-1}. Darker blue colours represent lower velocities close to 0 cms^{-1}. Note that the lowest velocities are in the parachute's wake, which is close to 0 cms^{-1}, while the fluid in fact speeds up near edges and the vent ring, reaching speeds more than 80000 cms^{-1}.

parachute, there is recirculation of air, which may have also contributed to instability and therefore resulting in the large lateral forces visible in Figure 6.

DISCUSSION

The objective of this paper was to analyse and evaluate the performance of a Ringsail parachute in Martian conditions for NASA's SRL through considering data such as the deceleration and drag, as well as how air flows around the parachute. A deceleration of 1308.89 ms^{-2} is extremely high for any spacecraft on Mars and could result in significant damage to the spacecraft. This value of deceleration means almost 130 g's of deceleration, which is far too high. Mars parachutes typically apply decelerations of around 5-10 g's. For example, Curiosity's parachute produced roughly 289 kN of drag (13), which ensured the safe landing of the Curiosity Rover. The coefficient of drag, 3.92, is also much higher than previous Mars missions where DGB parachutes were used.

However, these results are applicable to the impermeable parachute. Upon considering porosity, this value for drag coefficient comes down to about 0.96, which is a significantly more realistic drag coefficient, and aligns with previous studies such as (6) and (14). This reveals that the Ringsail design can be adopted for supersonic deceleration in the Martian atmosphere, and specifically for use in the Lander's mission with slight changes to porosity and sizing helping to obtain a drag coefficient for this parachute within the desired range of 0.5-0.8.

The proximity of this value to the desired drag coefficient provides hope that smaller Ringsail parachutes could potentially be developed for this and future Mars missions as the results suggest that the parachute could be within the 0.5-0.8 range if the drag force was slightly smaller. In fact, a previous study (14) most similar to this paper investigates the performance of a roughly 30 metre diameter SSRS parachute, whilst the parachute simulated in this research has a diameter 6 metres smaller. This paper therefore reveals that, since the smaller parachute examined is close to achieving a drag coefficient of 0.5-0.8, smaller SSRS

parachutes may be viable for Mars missions, saving costs and payload mass.

While the estimated drag coefficient is slightly higher, this could be due to software limitations. Fusion360 is relatively ineffective at meshing complex geometries and representing material porosity and Autodesk CFD is not able to mimic inflation dynamics, two factors which impact the performance of the parachute in the simulation. Although porosity was accounted for to some extent, inflation dynamics were unable to be included, leading to slightly less reliable results. Other similar studies tend to use custom coded CFD frameworks, such as NASA's LAVA Solver, which are more advanced and are able to handle more complex meshing and inflation dynamics. Therefore, future research on the suitability of the Ringsail parachute for supersonic, low-density conditions could be experimented using this more advanced software, or empirically through real-world tests, such as those conducted during the ASPIRE project.

Additionally, the presence of high-speed flow separation near the edges could lead to oscillations and violent shaking, especially as the separation is asymmetric. Instability in the Ringsail parachute was indicated by oscillating lateral aerodynamic forces (Fx, Fz) and asymmetric pressure distributions in the canopy region. However, this may also be due to the presence of recirculation of air due to the lack of porosity in the modelled canopy, therefore further research into how fluid dynamics are affected by porosity must be examined before claims are made regarding the stability of Ringsail parachutes.

CONCLUSION

In conclusion, preliminary results from this paper suggest that the Ringsail parachute, with an estimated drag coefficient of 0.96, could potentially be suitable for the descent of the Sample Retrieval Lander into Mars. As the first CFD-based Ringsail Mars test in student work, it provides evidence suggesting that, if further modified slightly, the Ringsail could be a possible alternative to the DGB parachute for Mars missions even beyond the Sample Retrieval Lander.

However, there are certain limitations to the study. As mentioned in the Discussion, the initial simulation lacks consideration of porosity and inflation dynamics. Certain simplification in the geometry of the parachute, such as the omission of suspension lines could have impacted the results slightly, potentially leading to more desirable and accurate drag coefficient values. Additionally, this paper utilised Autodesk CFD as opposed to more advanced software with increased meshing and solver capabilities. Despite these limitations, the findings of this paper may still be taken into consideration as a contribution to the development of a parachute for the SRL, as it provides a starting point, suggesting a parachute design, Ringsail, that could be applicable for this mission.

Future work should not only further refine these results by addressing these limitations, but could also explore possible changes that may enhance the performance of the Ringsail under Martian conditions. For example, different diameters and porosities could be tested and their effects on aerodynamic coefficients analyzed to investigate how the Ringsail could be optimized and improved further. Moreover, as mentioned in the Discussion, empirical data could be collected by running physical wind tunnel tests, which could also help to explore actual inflation dynamics. Perhaps a hybrid method could be implemented which considers both simulation and wind tunnel test data, which would also improve the reliability of data due to the increased ability to internally validate results. Future work may also want to consider methods to reduce costs for this mission, perhaps by reducing area and therefore fabric requirements, as NASA is currently facing a steep cost of roughly $11 billion USD for the whole mission (15), hence cost is an important factor to consider when deciding upon the parachute model.

CONFLICT OF INTERESTS

The author declares that there are no conflicts of interest regarding the publication of this article.

REFERENCES

1. Carney S. Sample Retrieval Lander [Internet]. NASA Science. 2024 [cited]. Available from: https://science.nasa.gov/mission/mars-sample-return/sample-retrieval-lander/#srl-tech-specs (accessed on 2025-05-13)
2. Corliss J, Edquist K. Mars Sample Return Sample Retrieval Lander (SRL) and Earth Entry Vehicle (EEV) [Internet]. 2021 Jul. Available from: https://ntrs.nasa.gov/api/citations/20210017965/downloads/2021_Summer_EDL_Seminar_MSR_FINAL%20v1.pdf (accessed on 2025-03-18)
3. Murrow H, McFall Jr J. Some test results from the NASA planetary entry parachute program. | Journal

of Spacecraft and Rockets. Journal of Spacecraft and Rockets [Internet]. 6(5). Available from: https://arc.aiaa.org/doi/abs/10.2514/3.29624?journalCode=jsr (accessed on 2025-05-13). https://doi.org/10.2514/3.29624

4. Bendura R, Huckins III E, Coltrane L. Performance of a 19.7 Meter Diameter Disk Gap Band Parachute in a Simulated Martian Environment [Internet]. 1968 Jan. Available from: https://ntrs.nasa.gov/api/citations/19680004328/downloads/19680004328.pdf
5. Bendura R, Lundstrom R, Renfroe P, LeCroy S. Flight Tests Of Viking Parachute System In Three Mach Number Regimes [Internet]. 1974 Nov. Available from: https://ntrs.nasa.gov/api/citations/19750002913/downloads/19750002913.pdf
6. Huang M, Wang W, Li J. Analysis and Verification of Aerodynamic Characteristics of Tianwen-1 Mars Parachute. Space: Science & Technology [Internet]. 2022 Jan; 2022. Available from: https://downloads.spj.sciencemag.org/space/2022/9805457.pdf (accessed on 2025-02-27). https://doi.org/10.34133/2022/9805457
7. Cruz J, Mineck R, Keller D, Bobskill M. Wind Tunnel Testing of Various Disk-Gap-Band Parachutes [Internet]. 2003 Jan. Available from: https://ntrs.nasa.gov/api/citations/20030064894/downloads/20030064894.pdf. https://doi.org/10.2514/6.2003-2129
8. Gallon J, Clark I, Rivellini T, Adams D. Low Density Supersonic Decelerator Parachute Decelerator System [Internet]. Nasa.gov. 2022. Available from: https://dataverse.jpl.nasa.gov/file.xhtml?fileId=51037&version=2.0 (accessed on 2025-03-13)
9. Xu X, Chen G, Zou T, Jia H, et al. Numerical study on aerodynamic characteristics of Mars parachute system with different combinations of fabric permeability and structural porosity. Aerospace Science and Technology [Internet]. 2024 Aug 2;153:109449. Available from: https://www.sciencedirect.com/science/article/abs/pii/S1270963824005807 (accessed on 2025-09-12). https://doi.org/10.1016/j.ast.2024.109449
10. Hu Y, Xu F, Gao Z. A Comparative Study of the Simulation Accuracy and Efficiency for the Urban Wind Environment Based on CFD Plug-Ins Integrated into Architectural Design Platforms. Buildings [Internet]. 2022 Sep 19; 12 (9): 1487. Available from: https://www.mdpi.com/2075-5309/12/9/1487 (accessed on 2025-10-10). https://doi.org/10.3390/buildings12091487
11. Huang D, Avery P, Farhat C, Rabinovitch J, Derkevorkian A, Peterson L. Modeling, simulation and validation of supersonic parachute inflation dynamics during Mars landing [Internet]. 2019 Dec. Available from: https://arxiv.org/pdf/1912.01658 (accessed on 2025-03-06)
12. Francois C, Jordan A, Michael B, Cetin K, Jonathan B. Simulating Supersonic Parachutes For Mars Entry, Descent & Landing [Internet]. 2022. Available from: https://ntrs.nasa.gov/api/citations/20220017102/downloads/Barad_ThA_65display_small.pdf (accessed on 2025-10-10)
13. NASA Jet Propulsion Laboratory. Mars Science Laboratory Parachute, Artist's Concept [Internet]. NASA Jet Propulsion Laboratory (JPL). 2011. Available from: https://www.jpl.nasa.gov/images/pia14836-mars-science-laboratory-parachute-artists-concept/ (accessed on 2025-09-13)
14. Cruz J, Snyder M. Estimates for the Aerodynamic Coefficients of Ringsail and Disk-Gap-Band Parachutes Operating on Mars [Internet]. 2017 Jun p.4-7. Available from: https://ntrs.nasa.gov/api/citations/20170005774/downloads/20170005774.pdf. https://doi.org/10.2514/6.2017-4055
15. Harwood W. NASA exploring 2 options to lower costs, speed up Mars Sample Return mission [Internet]. Cbsnews.com. CBS News; 2025. Available from: https://www.cbsnews.com/news/nasa-mars-sample-return-lower-cost-faster/ (accessed on 2025-08-17)
16. NASA's LDSD Project Completes Second Experimental Test Flight - NASA [Internet]. NASA. 2015. Available from: https://www.nasa.gov/news-release/nasas-ldsd-project-completes-second-experimental-test-flight/ (accessed on 2025-05-13)
17. Cruz J, Way D, Shinder J, Davis J. Reconstruction of the Mars Science Laboratory Parachute Performance and Comparison to the Descent Simulation [Internet]. 2013 Mar. Available from: https://ntrs.nasa.gov/api/citations/20130012763/downloads/20130012763.pdf. https://doi.org/10.2514/6.2013-1250
18. Muppidi S, O'Farrell C, Tanner C, Clark I. Modeling and Flight Performance of Supersonic Disk-Gap-Band Parachutes in Slender Body Wakes [Internet]. 2018 Jun. Available from: https://ntrs.nasa.gov/api/citations/20180007853/downloads/20180007853.pdf. https://doi.org/10.2514/6.2018-3623
19. Murrow H, Eckstrom C. Performance of disk-gap-band, ringsail, and cross parachutes at low earth altitudes | Journal of Spacecraft and Rockets. *Journal of Spacecraft and Rockets [Internet]*. 2025; 8 (4). Available from: https://arc.aiaa.org/doi/10.2514/3.30294 (accessed on 2025-05-13). https://doi.org/10.2514/3.30294
20. Narayana L, Ingenito A, Paolo Teofilatto. Large-Eddy Simulations of a Hypersonic Re-Entry Capsule Coupled with the Supersonic Disk-Gap-Band Parachute. Aerospace [Internet]. 2024 Jan 19 [cited 2025 Feb 21]; 11 (1): 94-4. Available from: https://doi.

org/10.3390/aerospace11010094.

21. Sengupta A, Steltzner A, Witkowski A, Candler G, Pantano C. Findings from the Supersonic Qualification Program of the Mars Science Laboratory Parachute System. 20th AIAA Aerodynamic Decelerator Systems Technology Conference and Seminar [Internet]. 2009 May 4; Available from: https://arc.aiaa.org/doi/10.2514/6.2009-2900 (accessed on 2025-04-15)
22. Siegel K, O'Farrell C, Rowan J, Peterson K, Lowry C. Preliminary Design of the Supersonic Disk-Gap-Band Parachute for Sample Retrieval Lander | AIAA Aviation Forum and ASCEND co-located Conference Proceedings. AIAA Aviation Forum and ASCEND co-located Conference Proceedings [Internet]. 2024; Available from: https://arc.aiaa.org/doi/10.2514/6.2024-4222 (accessed on 2025-05-13)
23. Tanner C, Clark I, Kushner L, Schairer E, Braun R. Aerodynamic Stability and Performance of Next-Generation Parachutes for Mars Descent [Internet]. Nasa.gov. 2022. Available from: https://dataverse.jpl.nasa.gov/file.xhtml?fileId=50939&version=2.0 (accessed on 2025-05-13)
24. Zang T, Dwyer-Cianciolo A, Kinney D, Howard A, et al. Overview of the NASA Entry, Descent and Landing Systems Analysis Study [Internet]. Available from: https://ntrs.nasa.gov/api/citations/20100033145/downloads/20100033145.pdf
25. Zumwalt C, Cruz J, Keller D. Wind Tunnel Test of Subscale Ringsail and Disk-Gap-Band Parachutes [Internet]. 2016 Jun. Available from: https://ntrs.nasa.gov/api/citations/20160010106/downloads/20160010106.pdf?form=MG0AV3. https://doi.org/10.2514/6.2016-3882